IOPscience iopscience.iop.org

Home Search Collections Journals About Contact us My IOPscience

Density profiles and correlation function of percolating clusters in finite strips

This article has been downloaded from IOPscience. Please scroll down to see the full text article.

1993 J. Phys. A: Math. Gen. 26 3955

(http://iopscience.iop.org/0305-4470/26/16/012)

View the table of contents for this issue, or go to the journal homepage for more

Download details:
IP Address: 171.66.16.68
The article was downloaded on 01/06/2010 at 19:25

Please note that terms and conditions apply.

J. Phys. A: Math. Gen. 26 (1993) 3955–3962. Printed in the UK

Density profiles and correlation function of percolating clusters in finite strips

R A Monetti and E V Albano

Instituto de Investigaciones Fisicoquímicas Teóricas y Aplicadas (INIFTA), Facultad de C. Exactas, Universidad Nacional de La Plata, Sucursal 4, Casilla de Correo 16, 1900 La Plata, Argentina

Received 16 December 1992

Abstract. The percolation model studied in finite strips ($L \ll M$) at criticality is characterized by the preferential growth of percolating clusters in the L-direction. In this work we present a Monte Carlo and finite-size scaling study of the density profiles of the percolating clusters. The behaviour of the pair-connectedness function is also analysed at criticality within both the algebraic and the exponential regimes.

1. Introduction

The study of percolation phenomena has attracted growing attention due to their relevance in many fields of physics and physical chemistry (for example, see the reviews [1–6] and references therein). It should be noted that most of the available work on percolation in two dimensions, performed using different techniques, has been done in a $L \times L$ geometry [1–6]. However, various authors have also considered the effect of non-quadratic shapes in percolation. For example, $L \times M$ and strip geometries have been studied by means of transfer matrix and phenomenological renormalization methods (see [7–11] and references therein). Furthermore, studies of other models in rectangular or strip geometries, such as for example the Ising model (see [12–14] and references therein), have demonstrated that this is a useful approach which may contribute to the understanding of the whole problem. In recent works [15, 16] we have analysed some aspects of the critical behaviour of the site percolation model on the square lattice in an $L \times M$ geometry. This geometry is particularly useful for the understanding of finite-size effects on the behaviour of adsorbed monolayers on stepped surfaces assuming random adsorption on terraces L-lattice spacing wide ($M \equiv$ step length) [12–17], as well as for diffusion and conduction processes in layered media [6].

At criticality and using free boundary conditions, due to the constrain $L \ll M$ one observes the growth of percolating clusters in the L-direction only [15]. Also, for a relatively small site occupation probability ($p = 0.5$), percolating clusters in the L-direction can be observed [15]. Therefore, in previous works we have analysed some relevant properties of the system such as the L- and M-dependence of both the critical probability and the percolation probability, the average number of percolating clusters (which is of the order of M/L), the cluster length distribution given by an exponential-exponential function, the average cluster length $\langle l \rangle \simeq 2L$, etc [15, 16].

Therefore, in this work we present a Monte Carlo and finite-size scaling study of the percolating clusters density profile and the pair-connectedness function in the M-direction. Density profiles are studied just at the critical point and also close to it.

0305-4470/93/163955+08$07.50 ©1993 IOP Publishing Ltd

The behaviour of the pair connectedness function is analysed at criticality within both the algebraic and the exponential regimes.

2. Theoretical background

Details on the site percolation model have already been published in various reviews [1-6], so they do not need to be repeated here. In the present work, the Monte Carlo simulations are performed using free boundary conditions in both the L- and M-directions; clusters are identified using standard algorithms and the results are typically averaged over 10^3-10^5 different configurations, depending on the lattice size, in order to achieve reasonable statistics [15, 16]. Since the study has always been performed under the constraint $L \ll M$, we refer to this geometry as 'finite strips'.

2.1. The density profile

One quantity of interest is the density profile of the percolating clusters in the L-direction defined as the probability $P(i, \xi, L, M)$ of a site located in the ith row parallel to the M-direction belonging to a percolating cluster, i.e.

$$P(i, \xi, L, M) = (pM)^{-1} \sum_{j=1}^{M} c(i,j) \qquad i = 1, L \tag{1}$$

where ξ is the correlation length, p is the occupation probability and $c(i,j) = 1$ ($c(i,j) = 0$) if the site $\{i,j\}$ belongs to a percolating cluster (otherwise). It is commonly known that close to the percolation threshold (p_c) and in the infinite-size limit the correlation length behaves as [1-6]

$$\xi \alpha |p - p_c|^{-\nu} \tag{2}$$

where ν is the correlation length exponent ($\nu = \frac{4}{3}$ in two dimensions [1-6]).

Close to p_c and for large lattices one expects that the density profile should be a homogeneous function, that is,

$$P(i, \xi, L, M) = L^x \bar{P}(i/L, \xi/L, L/M) \tag{3}$$

where the exponent x has to be determined and $\bar{P}(i/L, \xi/L, L/M)$ is a suitable scaling function.

For the used strip geometry the density profile becomes independent of M. So, using equation (2) one can rewrite equation (3) as

$$P(i, \xi, L) = L^x \bar{\bar{P}}[i/L, (p - p_c)L^{1/\nu}) \tag{4}$$

where $\bar{\bar{P}}$ is also a suitable scaling function.

On the other hand, the percolation probability $\Phi(p)$, i.e. the probability of a site belonging to a percolating cluster, can be written in terms of the density profile as

$$\Phi(p) = L^{-1} \sum_{i=1}^{L} P(i, \xi, L) = L^{x-1} \sum_{i=1}^{L} \bar{\bar{P}}[i/L, (p - p_c)L^{1/\nu}]. \tag{5}$$

The second summation can be put into integral form, that is,

$$\Phi(p) \propto L^{x-1} \int \bar{\bar{P}}[i/L, (p - p_c)L^{1/\nu}] \, di \tag{6}$$

and this integral can be expressed in terms of the variable $u = i/L$. Then

$$\Phi(p) \propto L^x \int \bar{P}[u, (p - p_c)L^{1/\nu}] \, du. \tag{7}$$

From finite-size scaling arguments it is known that at p_c and for large lattices $\Phi(p)$ behaves as

$$\Phi(p) \propto L^{-\beta/\nu} \tag{8}$$

where $\beta = \frac{5}{36}$ in two dimensions [1-6]. Now, comparing equations (7) and (8) it follows that $x = -\beta/\nu$, and therefore equation (4) becomes

$$P(i, \xi, L) = L^{-\beta/\nu} \bar{P}[i/L, (p - p_c)L^{1/\nu}]. \tag{9}$$

2.2. The pair-connectedness function at p_c

The pair-connectedness function is the probability that two sites at a distance r belong to the same cluster. Due to the geometry used ($L \ll M$) it is only interesting to study the pair-connectedness function calculated parallel to the M-direction on percolating clusters at p_c. According to finite-size scaling arguments, one has that close to p_c the pair-connectedness function $G(r, \xi, L, M)$ behaves as [1-6]

$$G(r, \xi, L, M) = L^{-\beta/\nu} g[r/L, (p - p_c)L^{1/\nu}, L/M] \tag{10}$$

where r is now the distance measured parallel to the M-direction and g is a suitable scaling function. In the limit $L \ll M$ the function g becomes independent of the aspect ratio L/M and also just at p_c the second variable vanishes, so equation (10) becomes

$$G(r, L) = L^{-\beta/\nu} g(r/L). \tag{11}$$

Note that in the thermodynamic limit one has $g(r/L) \propto (r/L)^{-\beta/\nu}$, so $G(r) \propto r^{-\beta/\nu}$. Then, for $r \ll L$, $G(r, L)$ exhibits the so-called algebraic behaviour [18], while for $L < r < M$ there appears an exponential decay of $G(r, L)$, namely

$$G(r, L) \propto L^{-\beta/\nu} \exp(-ar/L) \tag{12}$$

where a is a constant independent of L [18]. The physical interpretation of this crossover behaviour is the following [18]: what matters in the finite-size scaling of a system which is finite in all its dimensions is its smallest linear dimension (L). So, when criticality is approached, the correlation length grows uniformly until $\xi \simeq L$, then the system feels its finite size already very strongly and therefore ξ stays of the order of L throughout the critical region. Thus, $G(r, L)$ must have an exponential decay in the M-direction, with a correlation length proportional to L.

3. Results and discussion

3.1. The density profile

Figure 1(a) shows plots of density profiles versus $(i - L/2)$ obtained at p_c using lattices of different sizes. Due to the missing neighbour effect at $i = 1$ and $i = L$ (remember that free boundary conditions are assumed) the profiles are depleted close to those boundaries. This effect propagates into the bulk and the profiles are symmetric around $i = L/2$, as shown in figure 1(a). This fact can be understood because the correlation length ξ, which would become infinite in an infinite system at criticality, stays of the order of $\xi \simeq L$ in the present case due to the geometric constrain. Density profiles obtained for $p < p_c$ are also symmetric and peak at $i = L/2$. The occurrence of peaked rather than flattened profiles for the bulk of samples with $L = 100$ suggests that even far away from criticality (say $p = 0.50$) the correlation length is rather large. Because of the symmetry, the data corresponding to rows equidistant from $i = L/2$ are averaged

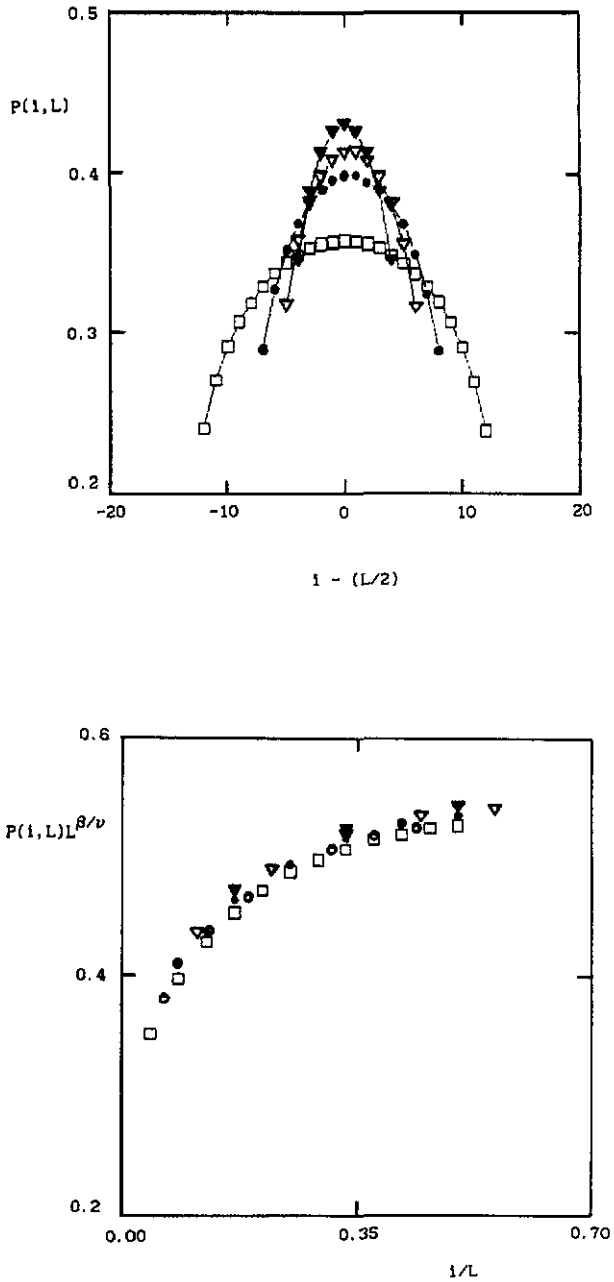

Figure 1. (*a*) Plots of the density profiles $P(i, L)$ versus $(i-L/2)$ for lattices of different sizes $(L\times M)$: ▼, 9×420; ▽, 12×440; ●, 16×576; □, 25×150. Lines have been drawn to guide the eye. (*b*) Plot of $P(i, L)L^{\beta/\nu}$ versus i/L for lattices of different sizes $(L\times M)$: ○, 16×576; ●, 12×440; ▽, 9×420; ▼, 6×200; □, 24×600. (*c*) Plot of $P(i/L, \Delta pL^{1/\nu})L^{\beta/\nu}$ versus i/L, with $\Delta pL^{1/\nu}=(p-p_c)L^{1/\nu}=0.24$, for lattices of different sizes $(L\times M)$: □, 15×120; ▼, 20×160; ●, 30×240; ▽, 25×200.

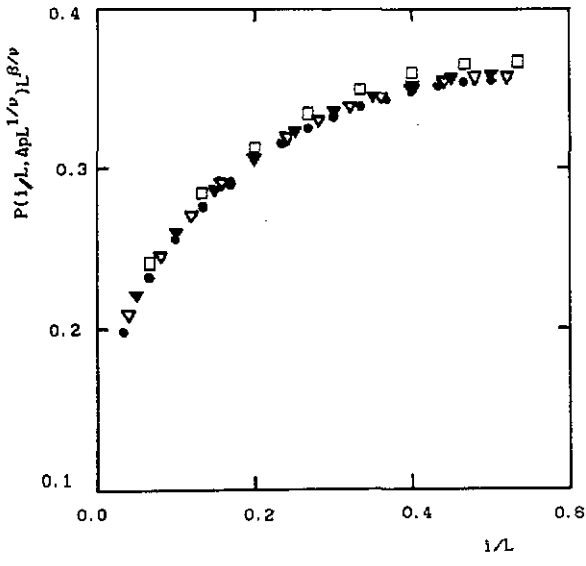

Figure 1. (continued)

over in the following. It should be noted that the order parameter profiles of the ferromagnetic Ising model in the absence of a magnetic field [12] (or equivalently the coverage profiles of the lattice gas model [13]) also exhibit a similar symmetry, but in contrast to the density profiles shown in figure 1(*a*) the former profiles smoothly flatten out close to the critical temperature.

In order to test the scaling hypothesis of equation (9), we first investigated just at criticality. In fact, at $p \equiv p_c$ the second variable vanishes and therefore it is convenient to make plots of $P(i, L)L^{\beta/\nu}$ versus i/L. As shown in figure 1(*b*), the collapsing of the data for lattices of different sizes is quite reasonable, taking into account the errors associated with the Monte Carlo simulation, and suggests that equation (9) should hold. However, a careful inspection of figure 1(*b*) shows the existence of a systematic deviation: the smaller the lattice width L the larger the value of $P(i, L)L^{\beta/\nu}$. This behaviour is not surprising since a similar deviation has been observed in a scaling study of the probability of a site belonging to a percolating cluster, which is related to the density profiles according to equations (5)–(8), and is due to a correction of the order of L^{-1} to the leading term [15].

Another possibility for testing equation (9) is to analyse the density profiles away from criticality but keeping constant the second scaling variable. Figure 1(*c*) shows plots of $P(i/L)L^{\beta/\nu}$ versus i/L for different lattice sizes with $p \neq p_c$ but obtained keeping $(p - p_c)L^{1/\nu} \equiv 0.24$ constant. Again, data collapsing on a single curve is observed, although a similar systematic deviation from that already discussed for figure 1(*b*) is also present.

Inspection of the collapsed density profiles shown in figures 1(*b*) and 1(*c*) suggests a parabolic symmetry around the maximum. In fact, close to the peak the data can be fitted by a curve of the form $(P_{max} - P)L^{\beta/\nu} \propto [\{(L/2) - i\}/L]^{\delta}$, with $\delta \simeq 1.8$. However, a better fit is obtained using a third-degree polynomial of the form $P \simeq 0.33 + 1.09 \times 2.1X^2 + 1.47X^3$, with $X = i/L$.

3.2. The pair-connectedness function at p_c

As it has already been pointed out in section 2 that two regimes are of particular interest in order to study the behaviour of the pair-connectedness function at p_c, namely the algebraic and exponential regions. Note that $G(r, L)$ is obtained by averaging over different i-values with $1 \leq i \leq L$.

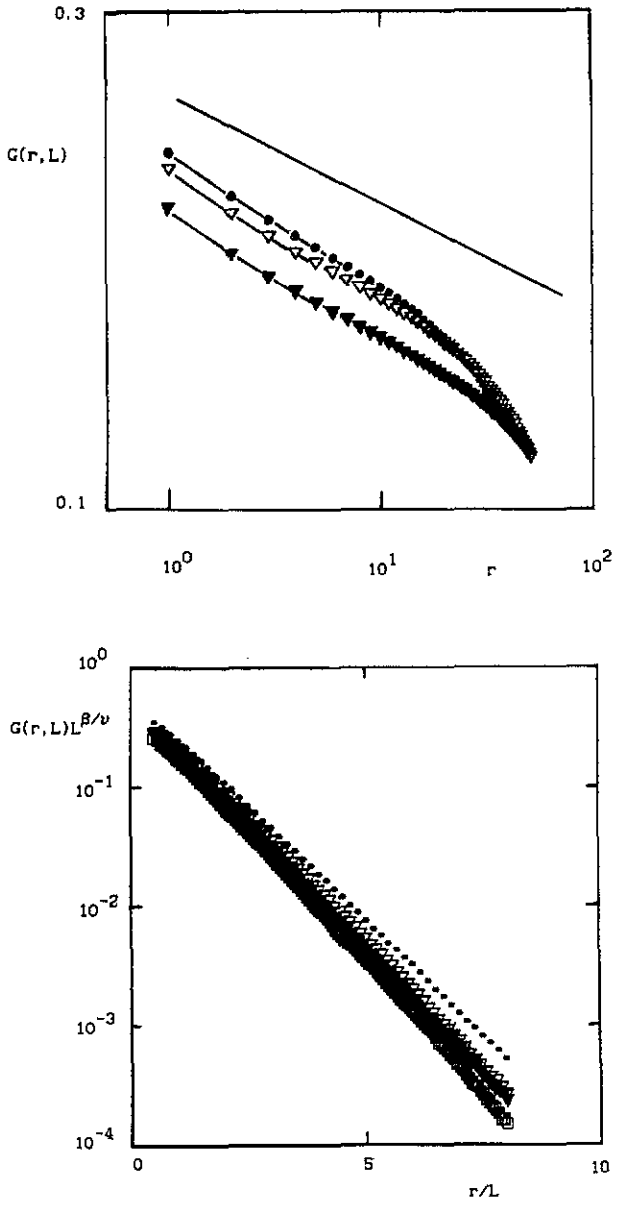

Figure 2. (*a*) Log-log plots of $G(r, L)$ versus r, within the algebraic regime ($r \ll L$), obtained for lattices of different sizes ($L \times M$): ●, 70×280; ▽, 100×300; ▼, 150×600. The straight line with slope $\beta/\nu = 5/48$ has been drawn for comparison. (b) Semilogarithmic plots of $G(r, L)L^{\beta/\nu}$ versus r/L, within the exponential regime ($L < r < M$), obtained with lattices of different sizes ($L \times M$): □, 16×384; ▽, 9×576; ▼, 12×384; ●, 6×420.

Figure 2(a) shows log–log plots of $G(r, L)$ versus r obtained for lattices of different sizes within the algebraic regime ($r \ll L$). According to equation (11) one should expect linear behaviour with an asymptotic slope given by $\beta/\nu = \frac{5}{48} \simeq 0.105$; nevertheless, from the straight lines of figure 2(a) we get $\beta/\nu \simeq 0.128 \pm 0.003$. A collapse of the data was attempted without success.

On the other hand, figure 2(b) shows semilogarithmic plots of $G(r, L)L^{\beta/\nu}$ versus r/L (see equation (12)) obtained with lattices of different sizes within the exponential regime ($L < r < M$). In spite of the fact that points corresponding to different lattices are on straight lines, the observed data collapsing is poor. Let us note that the value L/a which enters in the exponential part of equation (12) is the mean cluster length ($\langle l \rangle$), measured parallel to the M-direction [18].

From direct measurements of the cluster length distribution we have obtained $\langle l \rangle \simeq 2L$ [16]. On the other hand, from the slopes of the straight lines of figure 2(b) one gets a-values ranging from $a \simeq 0.38$ ($L = 6$, $M = 420$) to $a \simeq 0.46$ ($L = 24$, $M = 576$). This result suggests that in the asymptotic regime the expected value $a \simeq 0.5$ should be recovered.

It is interesting to note that the growth of percolating clusters in the L-direction, due to the constraint $L \ll M$, can be qualitatively compared with the development of domains of spins-up and spins-down crossing through the sample (L-direction), observed for the same geometry, working with the ferromagnetic Ising model in the absence of both bulk and surface fields [12–14]. From conformal invariance [19] and a Monte Carlo study of the exponential behaviour of the correlation function at criticality [12, 13], it follows that the average distance $\langle l_d \rangle$ between the border of domains with different spins is given by $\langle l_d \rangle = (\pi/2)^{-1} L$.

In order to understand the difference between the exponents β/ν evaluated using the data of figure 2(a) and the exact values, as well as the failure of the connectedness function data collapsing, it should be noted that some of the exponents which govern the bulk critical behaviour of certain properties may be different from those valid when approaching the surface of the cluster. For example, the intersection of a percolating cluster with a lattice surface strongly reduces the connectivity and causes the exponent $\beta = \frac{5}{36}$ to change into $\beta_s \simeq 0.398 \pm 0.005$ [20]. However, ν remains unchanged. In the present work the evaluation of the connectedness function in the M-direction involves averages over rows belonging not only to the bulk but also to the surfaces and close to them. Therefore, due to the contribution of the latter, the ratio β/ν which follows from figure 2(a) slightly overestimates the exact value. In view of this result, the dependence of β on the distance to the surface is being analysed. Preliminary results obtained evaluating the connectedness function for $i = 1$ give $\beta_s \simeq 0.40$, which is in agreement with [20].

On the other hand, the correction that one may introduce in the scaled form of the density profiles due to the change in β (equation (10)) appears to be irrelevant in view of the obtained data collapsing shown in figures 1(b) and 1(c).

4. Conclusions

The density profiles of percolating clusters in the L-direction and the pair-connectedness function of that clusters in the M-direction have been studied by means of the Monte Carlo method and discussed on the basis of finite-size scaling arguments. The missing neighbours at the edges of the lattice causes the connectivity to be reduced

and consequently the profiles become depleted close to this region. Profiles exhibit symmetry around the centre of the sample. The pair-connectedness function is studied within both the algebraic and the exponential regimes. Deviation from data collapsing is due to edge effects. The average cluster length (M-direction) evaluated within the exponential regime agrees with direct measurements made previously.

Acknowledgments

This work was financially supported by the Consejo Nacional de Investigaciones Científicas y Técnicas (CONICET) de la República Argentina. RAM gratefully acknowledge the Comisión de Investigaciones Científicas (CIC) de la Provincia de Buenos Aires (Argentina) for the provision of a fellowship. EVA would like to acknowledge stimulating discussions with Professor K Binder.

References

[1] Stauffer D 1979 *Phys. Rep.* **54** 1
[2] Stauffer D, Coniglio A and Adam A 1982 *Adv. Polymer Sci.* **44** 103
[3] Stauffer D 1985 *Introduction to Percolation Theory* (London: Taylor and Francis)
[4] Heermann H 1986 *Phys. Rep.* **136** 143
[5] Aharony A 1986 *Percolation* ed G Grinstein and G Mazenko (Singapore: World Scientific)
[6] Feders J 1988 *Fractals* (New York: Plenum)
[7] Derrida B and Vannimenus J 1980 *J. Physique* **41** L473
[8] Derrida B and De Seze L 1982 *J. Physique* **43** 475
[9] Nightingale P 1982 *J. Appl. Phys.* **53** 7927
[10] Normand J M, Herrmann H J and Hajjar M 1988 *J. Stat. Phys.* **52** 441
[11] Lam P M 1989 *J. Stat. Phys.* **54** 1081
[12] Albano E V, Binder K, Heermann D W and Paul W 1989 *Z. Phys.* B **77** 445
[13] Albano E V, Binder K, Heermann D W and Paul W 1989 *Surface Sci.* **223** 151
[14] Albano E V, Binder K, Heermann D W and Paul W 1989 *J. Chem. Phys.* **91** 3700
[15] Monetti R A and Albano E V 1991 *Z. Phys.* B **82** 129
[16] Monetti R A and Albano E V 1993 *Z. Phys.* B **90** 351
[17] Wagner H 1979 *Physical and Chemical Properties of Stepped Surfaces* (*Springer Tracts in Modern Physics* **85**) ed G Höhler (Berlin: Springer)
[18] Binder K 1990 *Finite Size Scaling and Numerical Simulation of Statistical Systems* ed V Privman (Singapore: World Scientific)
[19] Cardy J L 1984 *J. Phys. A: Math. Gen.* **17** L385; 1987 *Phase Transitions and Critical Phenomena* ed C Domb and J L Lebowitz, (New York: Academic) p 84
[20] Watson B P 1986 *Phys. Rev.* B **33** 6446